Hard Probes with the STAR Experiment

J.C. Dunlop[a](for the STAR* Collaboration)

[a]Physics Department,
Brookhaven National Laboratory,
Upton, NY 11973 U.S.A

Recent results on the use of hard probes in heavy ion collisions by the STAR experiment at RHIC are reviewed. The increased statistical reach from RHIC run 4 and utilization of the full capabilities of the STAR experiment have led to a qualitative improvement in these results. Light hadrons have been identified out to transverse momenta (p_T) of 12 GeV/c, allowing for clear identification of the dominant processes governing particle production in different p_T windows. Clean signatures of dijets have been seen even in central Au+Au collisions. Nuclear modification factors for non-photonic electrons, predominantly from the decay of heavy-flavored hadrons, have also been measured out to p_T of 8 GeV/c. For $p_T >\sim 6$ GeV/c, inclusive spectra of all charged hadrons, including heavy-flavored ones, appear to be suppressed equally strongly (by a factor of four to five) in central Au+Au collisions relative to p+p collisions; interestingly enough, the probability of finding a hadron from a dijet partner is suppressed to this same level.

1. Introduction

The use of hard probes in heavy ion collisions has shown itself to be highly successful in recent years. At mid-rapidity, high transverse momentum (p_T) particles are strongly suppressed, by a factor of four to five, in central Au+Au collisions relative to p+p collisions, and are not suppressed in d+Au collisions [1–3]. Away-side hadrons from partner dijets are also strongly suppressed in central Au+Au collisions, but not in d+Au collisions [3,4]. The standard explanation is that these phenomena are due to induced gluon radiation in a dense medium [5–8]. Within such approaches, the density needed to reproduce the data is large, about a factor of 50 beyond that of cold nuclear matter.

However, significant uncertainties remain in the determination of the density of the medium through these methods. For example, in the "quenching weights" framework, folded with a realistic geometrical picture of the overlap zone, the observable single-particle suppression shows a saturation with increasing density: beyond a certain density the suppression of light hadrons changes rather slowly with increasing density [9,10]. The observed suppression is deep within this saturated regime, which essentially limits such measurements to providing a lower bound on the density of the medium. More recent questions have arisen as to the contribution of *collisional* rather than radiative energy loss, especially to the energy loss of heavy quarks [11–13]. Other related questions are discussed

*For the full list of STAR authors and acknowledgements, see appendix 'Collaborations' of this volume

in STAR's recent critical assessment [14]. In order to decrease such uncertainties, more incisive experimental data is necessary.

STAR has begun a program to meet this challenge. First, the experiment is uniquely positioned to analyze correlations induced by dijets, due to its full azimuthal coverage. The measurement of dihadrons introduces different biases, both geometrical and fragmentation-induced, than that of inclusive spectra. Second, with the addition of the Time-of-Flight system (TOF) and Barrel Electromagnetic Calorimeter (BEMC), STAR is well-positioned to vary the coupling strength between the probe and the medium, which determines the strength of the geometric biases. The most dramatic such variation is to set the coupling to zero for the trigger particle in a dihadron measurement: this is the promise of photon-tagged correlations [15]. An intermediate variation is expected to be provided by charm and bottom quarks; due to their mass, it has been predicted that the radiative energy loss of such quarks is decreased in medium relative to that of light quarks [16–18]. The combination of all these different biases leads to different dependences of the suppression on density for the different measurements, and so it is hoped that the combination of the measurements will provide a precise measurement of the density of the medium.

2. Datasets

There have been five RHIC runs to date. Run 4, in 2004, focused on high statistics measurements in Au+Au at the top collision energy, $\sqrt{s_{NN}} = 200$ GeV, along with a smaller set of measurements at $\sqrt{s_{NN}}$ of 62.4, and a short polarized proton run at $\sqrt{s} = 200$ GeV. Roughly an order of magnitude more events from $\sqrt{s} = 200$ GeV Au+Au collisions were collected in run 4 than in the earlier run 2. Run 5, in 2005, focused on measurements in the smaller Cu+Cu system at $\sqrt{s_{NN}}$ of 200, 62.4, and 22 GeV, along with a longer run with polarized protons at $\sqrt{s} = 200$ GeV. Approximately half of the full-energy Au+Au data from run 4 has been fully reconstructed, along with approximately one-fifth of the full-energy Cu+Cu data from run 5. Preliminary results from these datasets were first presented at this conference.

The STAR experiment has been described in detail elsewhere [19]. In runs 4 and 5, significant upgrades were in place. A large fraction of the BEMC was fully commissioned and active, covering the full azimuth for pseudorapidity (η) $0 < \eta < 1$. The BEMC, when combined with the main tracking detector, the Time Projection Chamber (TPC), enables the measurement of electrons and photons out to high transverse momentum. As in run 3, in which the ions collided were d+Au, a trigger on high energy in a given calorimeter tower (high tower) was active, greatly increasing the capability of the detector to sample the RHIC luminosity and so increasing the p_T reach of the measurements. Also, as in run 3, a small TOF patch, a prototype of the upcoming upgrade to a full barrel TOF, was in place. When combined with the specific ionization (dE/dx) in the TPC, the TOF patch enables measurements of electrons at intermediate p_T [20] and identification of pions and protons from low p_T ($<\sim 0.5$ GeV/c) out to $p_T >\sim 12$ GeV/c [21].

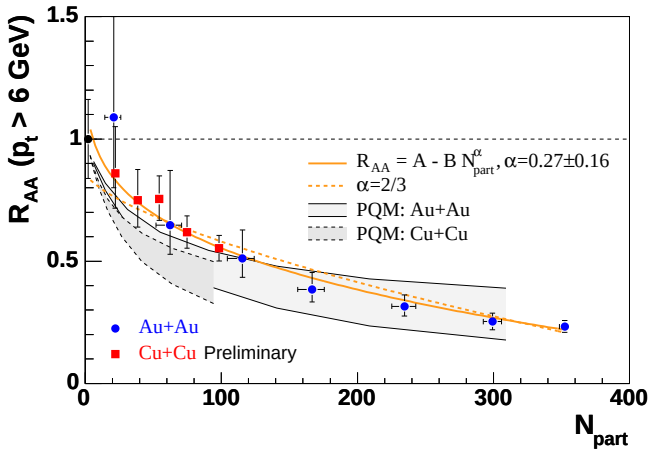

Figure 1. Nuclear modification factor R_{AA} for charged hadrons as a function of N_{part}. Au+Au results from ref. [2] are shown in blue, while Cu+Cu results are shown in red. Uncertainties shown are statistical and point-to-point systematic. Common uncertainties due to the p+p dataset are shown on the p+p point at left. PQM predictions are based on ref. [9].

3. Cu+Cu

As one test of the radiative energy loss picture, in run 5 RHIC ran collisions of the lighter system Cu+Cu. A lighter system brings the advantage that the nuclear overlap integral T_{AB} is more precisely determined at low N_{part} than in a heavier system. Fig. 1 shows the results for the nuclear modification factor R_{AA}, defined as $(dN/dp_T)_{AA}/(T_{AB}(d\sigma/dp_T)_{pp})$, for $p_T > 6$ GeV/c, as a function of N_{part}. Uncertainties for Au+Au and Cu+Cu datapoints are dominated by uncertainties in Glauber calculations of T_{AB}[22], while the common uncertainties from the p+p dataset [2] are placed on the p+p point on the left. The data show a clear and common evolution with increasing N_{part}: for a given N_{part}, R_{AA} is equivalent across systems, though with higher precision in Cu+Cu. Also shown are phenomenological fits to characterize the N_{part} dependence of R_{AA}. The data prefer a reduction with the power of $N_{part}^{1/3}$, though the more commonly expected $N_{part}^{2/3}$ reduction [23] is not strongly excluded. This scaling behaviour is a result of a complicated convolution of the spectral shape and collision geometry. The grey bands indicate the results of a full calculation incorporating such effects [9], which reproduces the common suppression in Cu+Cu and Au+Au at the same N_{part} but gives slightly larger suppression at low N_{part} than observed in the data.

4. Baryon enhancement at intermediate p_T

It has been known for some time now that at intermediate p_T ($p_T <\sim 6$ GeV/c) baryons behave differently in heavy ion collisions than mesons [24]. This is shown clearly by figure 2(a), which shows the ratio of proton to pion spectra in both central Au+Au

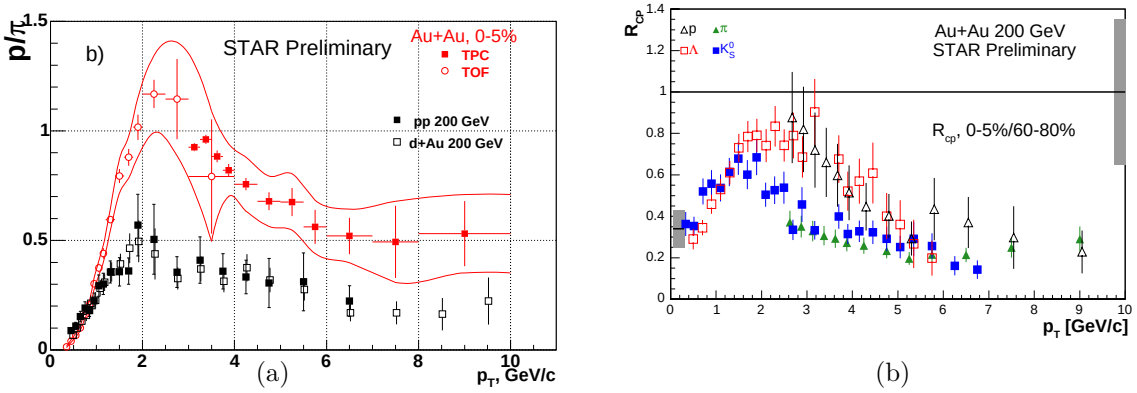

Figure 2. (a) Proton to π ratio as a function of p_T for central 0-5% Au+Au collisions and p+p collisions. For Au+Au, error bars are statistical and error bands systematic uncertainties. For p+p, error bars are combined statistical and systematic. For further details, see ref. [25].(b) R_{CP} as a function of p_T for identified particles. Errors are statistical and systematic, while the grey band at the right denotes common scale uncertainties from N_{binary}. See ref. [25] and [26] for more details.

collisions and in p+p collisions. The large enhancement in Au+Au collisions of the ratio at intermediate p_T indicates that the dominant source of particle production in this p_T range is not jet fragmentation in vacuum. With the high statistics of run 4 and the full utilization of STAR's capabilities, this enhancement is found to peak for $p_T \sim$ 2-3 GeV/c, beyond which the ratio falls towards the ratio in p+p collisions, though with the current uncertainties it is difficult to state conclusively if the ratio in Au+Au reaches that seen in p+p.

This enhancement also shows itself in the nuclear modification factor R_{CP}, the ratio between central and peripheral Au+Au collisions of N_{binary}-scaled spectra. Results for R_{cp} are shown in figure 2(b). As with v_2 [27,28], R_{CP} separates into two groups, baryons and mesons. The ϕ [29] and K^* [30], mesons with masses similar to the proton, follow the behavior of the mesons, proving that this separation is not due to mass. Such common grouping is violated in R_{AA}, in which the reference is from p+p collisions rather than peripheral collisions: strong enhancement in strange baryon R_{AA} is seen at intermediate p_T, with increasing enhancement for increasing strangeness content [26]. There were indications in previous results that these dependences on hadron species disappeared at high p_T [24], but the increased reach of the run 4 dataset strengthens this conclusion, placing the application of models incorporating parton energy loss on solid ground for $p_T >\sim$ 6 GeV/c.

5. Heavy Flavor

The sector of charm and bottom hadrons is also accessible using the identification capabilities of STAR. At this conference, we reported the first direct reconstruction of D

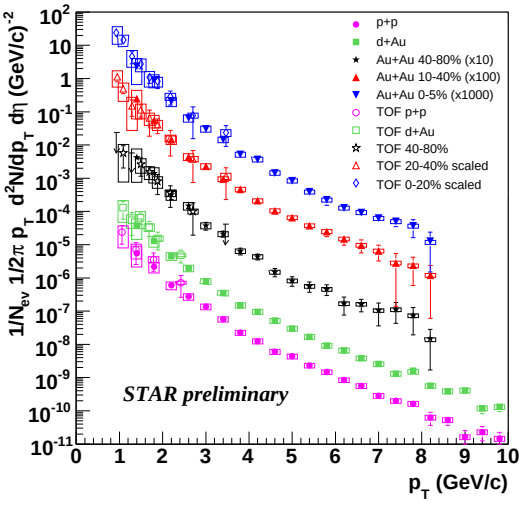

Figure 3. Invariant differential yield vs. p_T of non-photonic electrons. Error bars are statistical, and boxes denote systematic uncertainties. Spectra from 0-20% and 20-40% Au+Au collisions, measured by the TOF, have been scaled by $< N_{binary} >$ to match the centrality classes of the spectra from the BEMC (0-5% and 10-40%, respectively). See ref. [31] and [33] for more details.

mesons in Au+Au collisions [31]. Electrons can also be identified by using a combination of the TPC dE/dx, the TOF patch, and the BEMC. The dominant source of electrons in the detector is conversion of the photon daughters of π^0 and η hadrons in the detector material, along with Dalitz decays of these hadrons. This "photonic" source can be subtracted using an invariant mass technique. The resulting "non-photonic" electrons are expected to be predominantly from the decay of charm and bottom mesons. Figure 3 shows the resulting non-photonic electron spectra in p+p, d+Au, and Au+Au collisions. The contribution to the electrons of charm relative to bottom is expected to decrease with increasing p_T, though without direct measurement of the hadrons the point at which bottom dominates is somewhat uncertain [32]. Since the radiative coupling of heavy quarks to the medium is expected to be smaller than that of light quarks, due to their mass, the measurement of nuclear modification of heavy quarks is a sensitive test of the picture of radiative energy loss.

The total cross-section of charm production, determined predominantly by the direct measurement of D hadrons at low p_T, is found to scale with $< N_{binary} >$, as expected for a hard probe produced in the initial stages of the collision. More differentially, figure 4 shows the nuclear modification factor R_{AA} for D^0 mesons and non-photonic electrons as a function of p_T out to 8 GeV/c. For central Au+Au collisions, for $p_T >\sim 6$ GeV/c, R_{AA} for non-photonic electrons is rather similar to that measured for charged hadrons (figure 1). This measurement stands in contrast to the predictions before the conference of R_{AA} ~0.5-0.6 in this p_T range. For extreme medium densities ($dN/dy_{gluon} = 3500$ [18] or $\hat{q} = 14$ GeV^2/fm [17]), this large level of suppression can be reproduced within the

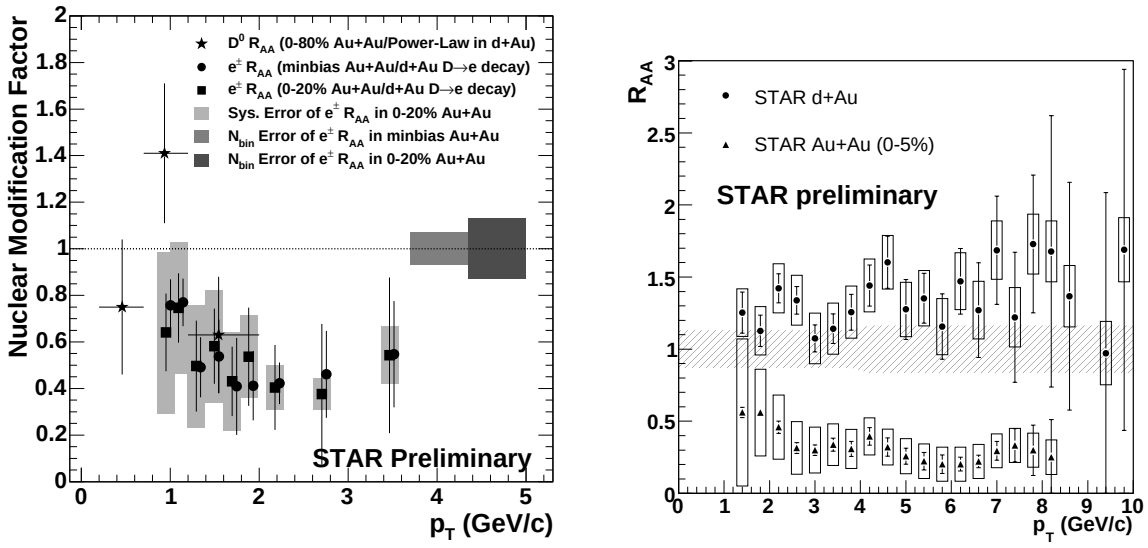

Figure 4. R_{AB} as a function of p_T for D^0 and non-photonic electrons. (a) D^0 and non-photonic electrons using the TOF. See ref. [31] for more details. (b) Non-photonic electrons using the BEMC. Error bars are statistical, error boxes point-to-point systematic uncertainties, and the band at unity denotes normalization uncertainty. See ref. [33] for more details.

radiative framework, but only if the bottom contribution is assumed to be negligible. Resolving whether this is a viable solution will depend on direct measurement of the charm and bottom contributions separately. Detector upgrades towards this goal are under active investigation [34].

6. Dijet Correlations

Dihadron correlations provide an alternative method to probe the medium than single-particle spectra, with some advantages. No Glauber calculation is required for the measurement of suppression, and geometric and fragmentation biases are different than those for single particles. However, previous analyses [4,37] have been limited by statistics to the intermediate p_T regime, where combinatoric backgrounds are high and multiple contributions unrelated to jet fragmentation are present. The increased statistics and experimental capabilities of the year 4 dataset have allowed STAR to increase the p_T scale and substantially reduce these issues.

Figure 5 shows per-trigger dihadron azimuthal correlations, in which both the trigger and associated particle are charged hadrons and the yield is normalized to the number of triggers. The trigger hadron has $8 < p_T < 15$ GeV/c. No background subtraction is performed in these plots. Both near-side (around $\Delta\phi = 0$) and away-side (around $\Delta\phi = \pi$) peaks are visible, and for the highest associated p_T combinatoric background is negligible. Little modification is apparent in the shape of the peaks, though the height of the away-side peak shows a clear suppression in central Au+Au collisions relative to d+Au

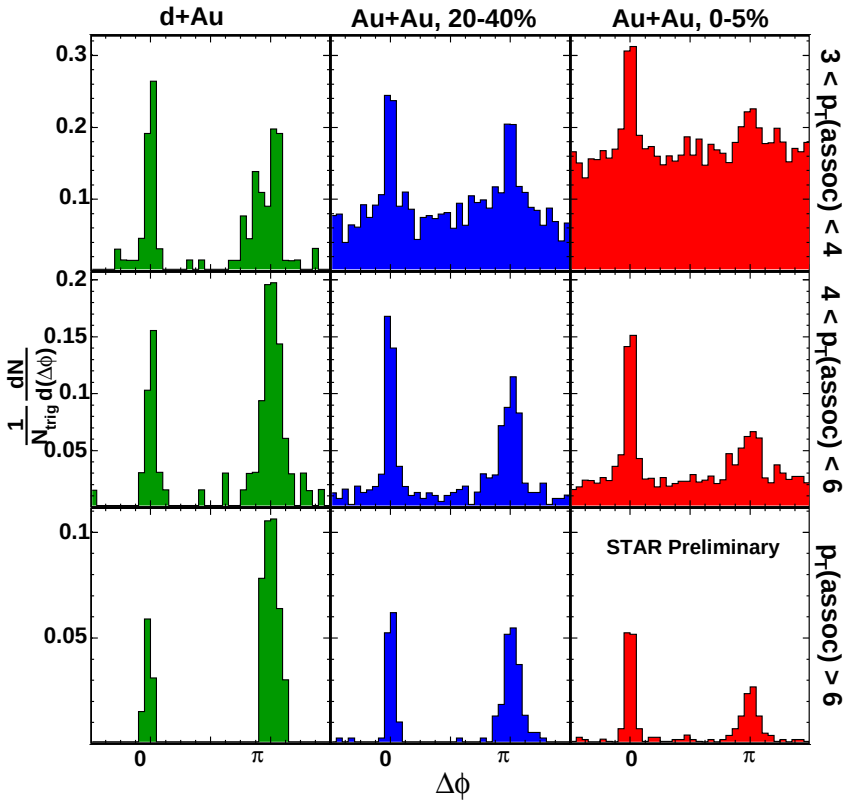

Figure 5. Per-trigger azimuthal correlations of charged hadrons associated with a charged hadron trigger with $8 < p_T < 15$ GeV/c. See ref. [40] for more details.

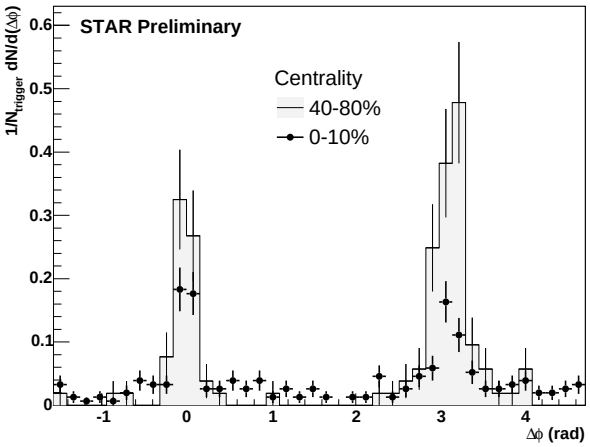

Figure 6. Per-trigger azimuthal correlations of charged hadrons associated with a trigger photon. The trigger photon has $E_T > 10$ GeV/c, while associated charged hadrons have $4 < p_T^{assoc} < E_T^{trigger}$. See ref. [39] for more details.

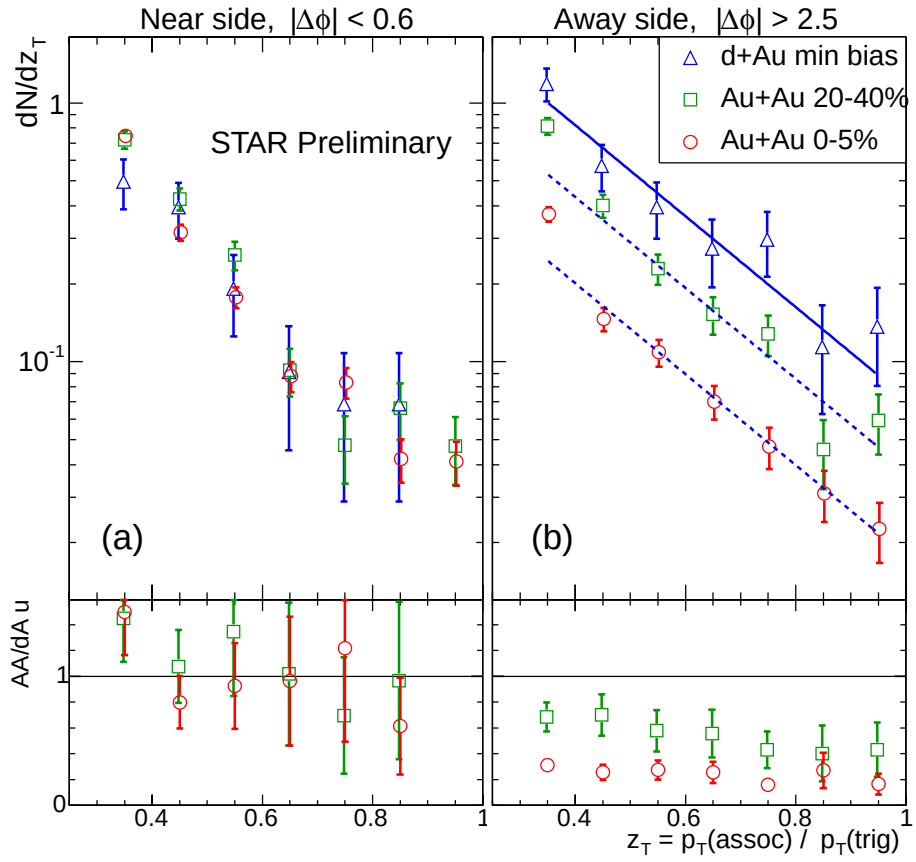

Figure 7. Top: Dihadron fragmentation functions as a function of z_T, for (a) near-side and (b) away-side. The solid line is an exponential fit of the z_T distribution for d+Au; the dashed lines are scaled by a factor 0.54(0.25) for 20-40% (0-5%) Au+Au. Bottom: ratio of dihadron fragmentation functions Au+Au/d+Au. See ref. [40] for more details.

collisions. These results stand in contrast to previous results in central Au+Au collisions: for intermediate thresholds, no significant strength was found in the away-side peak [4], while for extremely low thresholds strong modification in both the shape and strength were observed [37]. Unambiguously, these dihadron correlations reflect dijet phenomena in central Au+Au collisions.

Figure 6 shows a related correlation, in which the charged hadron trigger has been replaced by a photon detected in the BEMC. Here the trigger photon has $E_T > 10$ GeV/c, and the associated charged hadron has 4 GeV/c $< p_T < E_T^{trigger}$. For these E_T, photons are expected to come both from fragmentation (through the decay of π^0) and directly from the source [38]. In contrast to the charged-charged correlations, in the photon-charged correlation the strength of the near-side peak decreases from peripheral to central Au+Au collisions. This may reflect a relative increase in the contribution of direct photons to the trigger particles in central collisions [39]. This measurement represents a first step towards the ultimate goal of the direct measurement of the medium modification

of the fragmentation function using direct photon-tagged hadrons.

With the clean correlation peaks of figure 5, one can form a dihadron "fragmentation function", as proposed in ref. [41]. Results are shown in figure 7. The correlations are first binned in $z_T = p_T^{assoc}/p_T^{trigger}$, and then the peaks on the near and away side are integrated. While the strength of the near-side peak shows little modification from d+Au to central Au+Au collisions, the away-side peak shows a strong suppression, essentially independent of z_T for large z_T. Dihadrons incorporate a completely different set of biases than single-particle spectra, yet the level of suppression is similar to that seen for all single-particle spectra, by a factor of four to five. This similarity will place strong constraints on the medium density inferred from energy-loss calculations, and may enable the placement of an upper bound on the medium density. It has been proposed that from such an upper bound, combined with a lower bound on the entropy density, a lower bound on the number of degrees of freedom of the medium can be obtained [42].

7. Conclusion

Increased statistics and detector capability in run 4 have led to a qualitative improvement in the use of hard probes in STAR. Light hadron as well as non-photonic electron spectra have been measured to p_T of up to 10 GeV/c: the surprising result is that all hadrons, including those with heavy flavor, appear to be suppressed to the same level in Au+Au collisions. Dihadron correlations have moved into the precision regime with clear dijet signatures, and the beginning of the photon-jet program. Interestingly, dihadron correlations, which are affected by very different biases than single particle spectra, show the same level of suppression as single particle spectra. With these results, and with more to come from the full analysis of the current dataset and future datasets, it may be possible to move the determination of the properties of the medium created at RHIC into the precision phase.

REFERENCES

1. C. Adler *et al.* [STAR Collaboration], Phys. Rev. Lett. **89** (2002) 202301.
2. J. Adams *et al.* [STAR Collaboration], Phys. Rev. Lett. **91** (2003) 172302.
3. J. Adams *et al.* [STAR Collaboration], Phys. Rev. Lett. **91** (2003) 072304.
4. C. Adler *et al.* [STAR Collaboration], Phys. Rev. Lett. **90** (2003) 082302.
5. M. Gyulassy, P. Levai and I. Vitev, Nucl. Phys. A661 (1999) 637; M. Gyulassy, P. Levai and I. Vitev, Nucl. Phys. B571 (2000) 197; M. Gyulassy, P. Levai and I. Vitev, Phys. Rev. Lett. 85 (2000) 5535; M. Gyulassy, P. Levai and I. Vitev, Nucl. Phys. B594 (2001) 371.
6. E. Wang and X.N. Wang, Phys. Rev. Lett. 87 (2001) 142301.
7. R. Baier, Y.L. Dokshitzer, A.H. Mueller, S. Peigne and D. Schiff, Nucl. Phys. B483 (1997) 291; R. Baier, Y.L. Dokshitzer, A.H. Mueller and D. Schiff, Nucl. Phys. B531 (1998) 403; R. Baier, Y.L. Dokshitzer, A.H. Mueller and D. Schiff, Phys. Rev. C60 (1999) 064902; R. Baier, Y.L. Dokshitzer, A.H. Mueller and D. Schiff, JHEP 0109 (2001) 033.
8. U.A. Wiedemann, Nucl. Phys. B588 (2000) 303; U.A. Wiedemann, Nucl. Phys. A690

(2001) 731; C.A. Salgado and U.A. Wiedemann, Phys. Rev. Lett. 89 (2002) 092303; C.A. Salgado, U.A. Wiedemann, Phys. Rev. D68 (2003) 014008.
9. A. Dainese, C. Loizides and G. Paic, Eur. Phys. J. C **38** (2005) 461.
10. K. J. Eskola, H. Honkanen, C. A. Salgado and U. A. Wiedemann, Nucl. Phys. A **747** (2005) 511.
11. H. van Hees and R. Rapp, Phys. Rev. C **71** (2005) 034907.
12. G. D. Moore and D. Teaney, Phys. Rev. C **71** (2005) 064904.
13. M. G. Mustafa, Phys. Rev. C **72** (2005) 014905.
14. J. Adams *et al.* [STAR Collaboration], Nucl. Phys. A **757** (2005) 102.
15. X. N. Wang, Z. Huang and I. Sarcevic, Phys. Rev. Lett. **77** (1996) 231.
16. Y. L. Dokshitzer and D. E. Kharzeev, Phys. Lett. B **519**, 199 (2001).
17. N. Armesto, A. Dainese, C. A. Salgado and U. A. Wiedemann, Phys. Rev. D **71** (2005) 054027; private communication.
18. M. Djordjevic, M. Gyulassy, R. Vogt and S. Wicks, arXiv:nucl-th/0507019.
19. K.H. Ackermann et al., Nucl. Instrum. Methods A499 (2003) 624.
20. J. Adams *et al.* [STAR Collaboration], Phys. Rev. Lett. **94** (2005) 062301.
21. M. Shao, O. Barannikova, X. Dong, Y. Fisyak, L. Ruan, P. Sorensen and Z. Xu, arXiv:nucl-ex/0505026.
22. J. Adams *et al.* [STAR Collaboration], arXiv:nucl-ex/0311017.
23. I. Vitev and M. Gyulassy, Phys. Rev. Lett. **89** (2002) 252301; private communication.
24. J. Adams *et al.* [STAR Collaboration], Phys. Rev. Lett. **92**, 052302 (2004).
25. O. Barannikova *et al.* [STAR Collaboration], these proceedings.
26. S. Salur *et al.* [STAR Collaboration], these proceedings.
27. F. Wang *et al.* [STAR Collaboration], these proceedings.
28. M. Oldenburg *et al.* [STAR Collaboration], these proceedings.
29. X.Z. Cai *et al.* [STAR Collaboration], these proceedings.
30. J. Adams *et al.* [STAR Collaboration], Phys. Rev. C **71** (2005) 064902.
31. H. Zhang *et al.* [STAR Collaboration], these proceedings.
32. M. Cacciari, P. Nason and R. Vogt, arXiv:hep-ph/0502203; R. Vogt, these proceedings.
33. J. Bielcik *et al.* [STAR Collaboration], these proceedings.
34. K. Schweda *et al.* [STAR Collaboration], these proceedings.
35. Z. w. Lin and D. Molnar, Phys. Rev. C **68** (2003) 044901.
36. V. Greco, C. M. Ko and R. Rapp, Phys. Lett. B **595** (2004) 202.
37. J. Adams *et al.* [STAR Collaboration], Phys. Rev. Lett. **95** (2005) 152301.
38. K. Filimonov, arXiv:nucl-ex/0505008.
39. T. Dietel *et al.* [STAR Collaboration], these proceedings.
40. D. Magestro *et al.* [STAR Collaboration], these proceedings.
41. X. N. Wang, Phys. Lett. B **595** (2004) 165.
42. B. Muller and K. Rajagopal, arXiv:hep-ph/0502174.